International Journal of Tryptophan Research

ORIGINAL RESEARCH

Characterization of the Kynurenine Pathway and Quinolinic Acid Production in Macaque Macrophages

Chai K. Lim[1,2], Margaret M.C. Yap[3], Stephen J. Kent[4], Gabriel Gras[5], Boubekeur Samah[5], Jane C. Batten[4], Robert De Rose[4], Benjamin Heng[2], Bruce J. Brew[3,6] and Gilles J. Guillemin[1,2]

[1]Department of Pharmacology, School of Medical Sciences, University of New South Wales, Sydney, Australia. [2]MND and Neurodegenerative disease Research Group, Australian School of Advance Medicine, Macquarie University, Australia. [3]Applied Neurosciences, St. Vincent's Center for Applied Medical Research, Sydney, Australia. [4]Department of Microbiology and Immunology, University of Melbourne, Parkville, Victoria, Australia. [5]Laboratoire de Neuro-Immuno-Virologie, Service de Neurovirologie UMR E-01 CEA, France and UMR E1, School of Medicine, University Paris South 11, Le Kremlin-Bicêtre, France. [6]Department of Neurology, St. Vincent's Hospital, Darlinghurst, Australia.
Corresponding author email: gilles.guillemin@mq.edu.au

Abstract: The kynurenine pathway (KP) and one of its end-products, the excitotoxin quinolinic acid (QUIN), are involved in the pathogenesis of several major neuroinflammatory brain diseases. A relevant animal model to study KP metabolism is now needed to assess whether intervention in this pathway may improve the outcome of such diseases. Humans and macaques share a very similar genetic makeup. In this study, we characterized the KP metabolism in macaque primary macrophages of three different species in comparison to human cells. We found that the KP profiles in simian macrophages were very similar to those in humans when challenged with inflammatory cytokines. Further, we found that macaque macrophages are capable of producing a pathophysiological concentration of QUIN. Our data validate the simian model as a relevant model to study the human cellular KP metabolism in the context of inflammation.

Keywords: simian macrophages, kynurenine pathway, indoleamine 2,3-dioxygenase, quinolinic acid

International Journal of Tryptophan Research 2013:6 7–19

doi: 10.4137/IJTR.S11789

This article is available from http://www.la-press.com.

Introduction

The kynurenine pathway (KP; Fig. 1) is a major degradative metabolic route for the essential amino acid tryptophan (TRP), leading to the production of nicotinamide adenine dinucleotide (NAD), a crucial co-factor for many cellular functions.[1] In the last decade, the KP has emerged as a key regulator of the immune response. Munn and Mellor first described that TRP catabolism, through activation of the enzyme indoleamine 2,3-dioxygenase (IDO-1), is directly associated with immune tolerance.[2] KP activation also leads to the production of a cascade of downstream neuroactive metabolites. We, and others, showed previously that IDO-1 activation in human primary macrophages with IFN-γ leads to production of a pathophysiological concentration of the excitotoxic KP metabolite, quinolinic acid (QUIN),[3,4] being both neurotoxic and gliotoxic.[5–8] Based upon the literature, extensive studies have been conducted to examine the KP in various monocytic lineages, especially macrophages and microglia. These cells express all the KP enzymes and were consistently used as *in vitro* models to study the KP metabolism in immune-related pathology.

When it comes to the study of KP *in vivo* using animal models, a key concern is that KP metabolism varies between species. It is still unclear which animal models are relevant to the study of KP metabolism in relation to human pathology. Several earlier

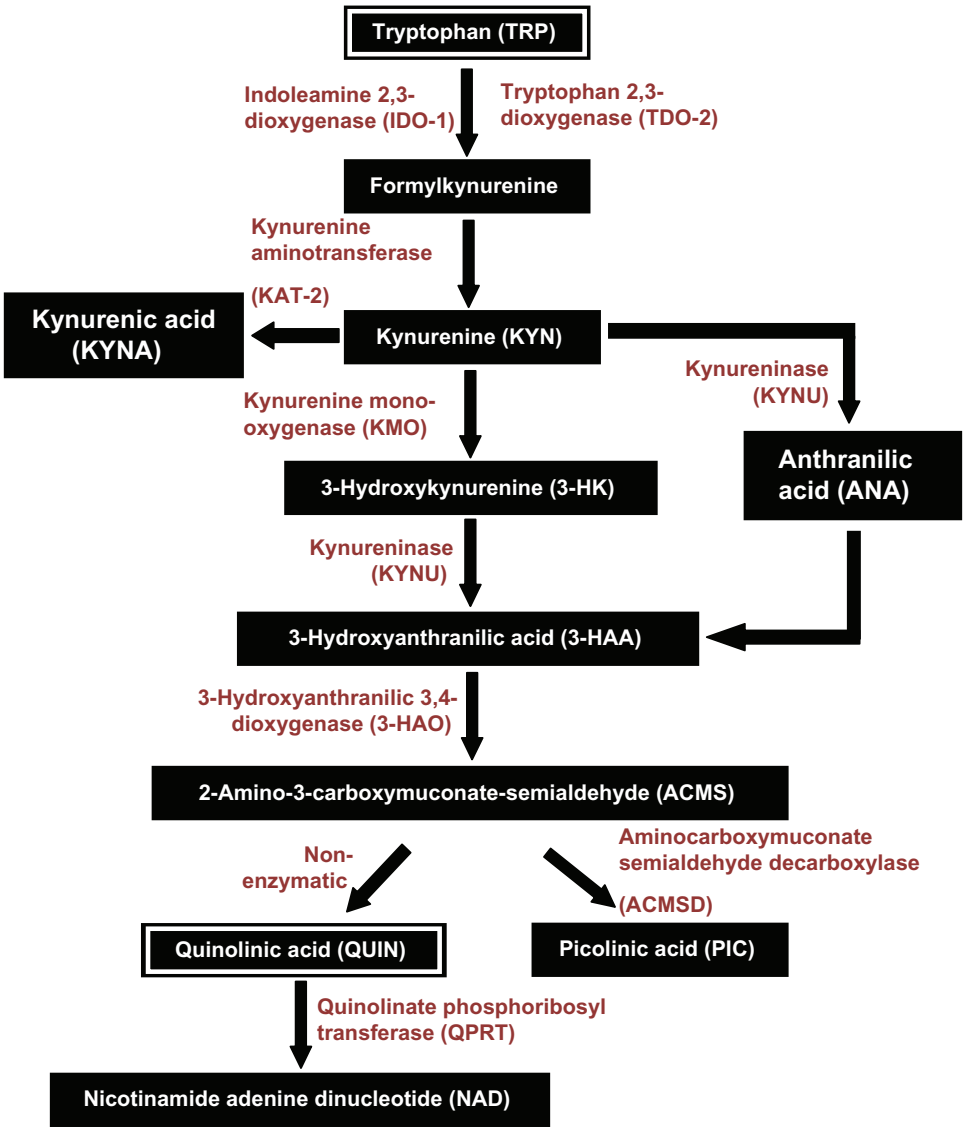

Figure 1. Simplified version of the kynurenine pathway.

studies have reported that in physiological conditions, activities of the KP enzymes in tissues, such as liver and kidney, were significantly different between species.[9–11] These comparisons include humans, macaques,[12] gerbils,[13] rabbits, rats, mice, and guinea pigs.[9,14] Not surprisingly, differences in the levels of KP metabolites between species have also been reported.[12] Regardless, studies looking at KP using animal models of various pathologies, such as rodent models, can still yield some significant outcomes. Studies involving central and systemic immune activation in mice,[15] macaques,[16] and gerbils[13] were able to replicate some clinical observations in patients with various neuropathological conditions. Some common trends included parallel responses in elevations of QUIN, concomitant KP metabolites, and markers of immune activation. Significant correlations between the severity of the neuropathology, levels of IFN-γ, the level of macrophages/microglia activation, IDO expression,[17] and QUIN accumulation[18] have been observed in SIV infected macaque models mimicking AIDS dementia complex (ADC).[19] This led us to think that the simian model is likely the most biologically relevant KP model to study human pathologies.

In this study we aim to characterize KP in simian primary macrophages in comparison to primary human cells by assessing the KP metabolic profile (enzymes and products) in response to immunological challenge (IFN-γ). Common macaque models studied in experimental research include the rhesus, cynomolgus, and pigtail macaque species.[20,21] The goal of this study is to ascertain whether these macaque species are relevant models to study KP in relation to various diseases, especially in the development and testing of novel therapies.

Materials and Methods

Human and animal ethics

All protocols in this study were approved by the Human Ethics Committees at the University of New South Wales, Animal Ethics Committees at the University of Melbourne and CSIRO animal health and Commissariat a l'énergie atomique (France). We studied blood samples from adult pigtail macaques (*Macaca nemestrina*),[21] cynomolgus macaques (*Macaca fascicularis*), and rhesus macaques (*Macaca mulatta*).

Reagents and chemicals

All cell culture media and supplements were from Life Technologies (CA, USA) unless otherwise stated. Chemicals for HPLC and GC/MS analysis were from Sigma Aldrich (St. Louis, MO, USA) unless otherwise stated.

Cell cultures

Human peripheral blood mononuclear cells (PBMC) were isolated from the blood of healthy volunteers (Australian Red Cross) using the density separation method with Ficoll-Paque (Pharmacia, Uppsala, Sweden) as previously described.[22] Monocyte-derived macrophages (MdM) were cultured using the classical adherence method. In brief, PBMCs were plated and adhered on modified surface (Falcon Primaria) plate (BD Biosciences, CA, USA) supplemented with 10% autologous human serum, 1% Glucose (AstraZeneca, NSW, Australia),1% Glutamax (100X), 1% Penicillin G/Streptomycin sulphate 100X Mix in RPMI medium. Cell cultures were maintained in a humidified atmosphere with 5% CO_2 at 37 °C. Adult macaque MdM were cultured from fresh blood using the method adapted from human MdM as described above. Highly purified macrophages were either stimulated with 100 IU/mL of IFN-γ or left unstimulated as controls for 24, 48 and 72 h. Trizol was then used to extract RNA. Each experiment was performed in triplicate.

Quantification of KP metabolites

TRP and KYN were concurrently measured using an Agilent 1200 series HPLC system (Santa Clara, CA, USA) as previously described with slight modification.[8] Cell culture supernatants were deproteinized with 10% TCA and passed through a 0.45 µm PTFE syringe filter (Waters Corp., MA, USA). Briefly, the standards and samples are applied to an Agilent Zorbax Eclipse XDB-C18 (5 µm, 150 × 4.6 i.d.) reverse phase column at an injection volume of 30 µL. The mobile phase consists of 0.1 M ammonia acetate at pH 4.65 pumped isocratically with a flow rate of 0.8 mL/min. TRP was quantified by fluorescence at an excitation wavelength of 254 nm and emission wavelength of 404 nm while KYN was detected using multi-wavelength detection at 365 nm. Read outs of the standards were expressed as peak area, which is used to plot the linear standard curve against

the known concentration of the standards used. Peak areas from samples were then interpolated from the standard curve to calculate the actual concentrations of TRP and KYN and expressed as μM.

PIC and QUIN were assayed using GC/MS in accordance with the method previously described.[23] Briefly, 50 μL of standards and samples were added to glass tubes with equal volumes of respective internal standards to the metabolites of interest. The mixtures were allowed to dry leaving residues, which were then allowed to derivatize with trifluoroacetic anhydride and hexafluoroispropanol to form the hexafluoroisopropyl ester of the respective acids. The final product was then dissolved in toluene, washed in sodium bicarbonate and ultrapure water prior to final filtrating through a miniature plastic column packed with silane treated glass wool and anhydrous sodium sulphate. The end product (1 μL) was injected into GC/MS for quantification operating in negative ionization mode. Concentrations of PIC and QUIN were calculated in two steps: firstly, the peak area ratio between the internal standards and its respective samples were determined; secondly, the ratios were then used to interpolate the concentrations of PIC and QUIN in the samples using the standard curve and expressed as μM.

Immunocytochemistry (ICC)

Human and pigtail macrophages stimulated with IFN-γ for 72 h were used for staining as previously described.[8] Our previous data indicated that IFN-γ stimulation for 24 and 48 h was not sufficient for KP assessment in terms of protein expression. Briefly, cells were seeded in Permanox chamber slides (Nunc, NY, USA) for up to 24 h. After treatment with IFN-γ for up to 72 h, cells were fixed with cold methanol/acetone (1:1; v/v) at –20 °C for 15 min. Fixatives were removed and thoroughly rinsed thrice with PBS. To facilitate access of antibodies into intracellular targets, membrane permeabilization was achieved with 10 min incubation in 0.025% Triton X-100 in PBS solution at ambient temperature (24 °C). Cells were allowed to block with 5% non-immune goat serum (NGS) diluted with PBS for at least 45 min at ambient temperature to minimize background in subsequent staining steps. The slides were divided equally into enclosed wells using PAP Pen (DAKO, Copenhagen, Denmark) upon removal of the blocking solution and immediately incubated with the respective primary monoclonal or polyclonal antibodies, diluted in 5% NGS solution, in each designated assigned wells for up to 1 h at 37 °C in a humidified chamber. Cells were then washed thoroughly with 5% NGS solution to remove excess unbound primary antibodies and incubated at 37 °C for another hour with the appropriate labeled secondary antibodies. Nuclear staining was performed using DAPI (Life Technologies) at 1 μg/mL for 5 min at ambient temperature. Finally, coverslips were mounted onto the slides with Fluoromount-G (Southern biotech, AL, USA) after removal of the secondary antibodies with several washes in PBS. Slides were then examined with an Olympus BX60 fluorescence microscope fitted with a SensiCam digital camera (Tokyo, Japan). Antibodies used in this study are detailed in Table 1.

Endpoint RT-PCR detection of mRNA expression of KP enzymes

The RT-PCR protocol was carried out as previously described.[6,8] The genetic sequences that were used for the KP enzymes were compared between the human and macaque rhesus (Table 2). The computationally predicted sequences showed that there was much similarity in sections of the sequences, even though human and macaque rhesus sequences were not exactly the same. Based on the close phylogenetic proximity of the three macaque species, sequences obtained for the macaque rhesus were considered as valid and representative for the pigtail and cynomolgus macaques. Primers were designed using the recently published macaque rhesus KP enzyme sequences. We then selected the best primer set out of four variants, determined by optimizing the hybridization temperature with Eppendorf gradient thermocycler (Hamburg, Germany) (Table 3A) followed by a run sequence outlined in Table 3B. Negative controls were (i) exclusion of target template, (ii) exclusion of reverse transcriptase, and (iii) genomic DNA. Amplicons were quantified using ImageJ (NIH; Rasband, W.S., ImageJ, U.S. National Institutes of Health, Bethesda, Maryland, USA, http://rsb.info.nih.gov/ij/, 1997–2008). Based on image analysis intensity ratio of the KP enzyme mRNA expressed relative to GAPDH mRNA, the standard error was between

Table 1. Details of primary and secondary antibodies used in immunocytochemistry.

Primary antibodies	Clonality	Isotype	Dilution	Company (Cat. #)	Secondary antibodies	Dilution
IDO-1	Monoclonal	IgG	1:200	Gift from O. Takikawa	Alexa fluor 594	1:400
TDO-2	Polyclonal	–	1:100	Gift from C. Miller	Alexa fluor 488	1:400
KAT-2/ AADAT	Polyclonal	–	1:100	Abnova (H00051166-A01)	Alexa fluor 488	1:400
KMO	Polyclonal	IgG	1:100	Abcam (ab93195)	Alexa fluor 594	1:400
KYNU	Polyclonal	–	1:100	Abnova (H00008942-A01)	Alexa fluor 488	1:400
QPRT	Monoclonal clone 5D11	IgG_1	1:200	Abnova (H00023475-M01)	Alexa fluor 594	1:400
ACMSD	Polyclonal	–	1:100	Abnova (H00130013-A01)	Alexa fluor 488	1:400
QUIN	Monoclonal	IgG	1:20	Millipore	Alexa fluor 594	1:400

Note: All secondary antibodies used in this study were purchased from Life Technologies.

5%–8%. Experiments were performed in triplicates for all samples.

Statistical analysis

All figures are presented with mean values and standard errors using GraphPad Prism 5. Statistical analysis was performed using paired *t*-test with two-tailed distribution for single pair-wise comparison while multi-variant comparison was performed using one-way ANOVA with Dunnett's post-hoc analysis. A P value of <0.05 was considered to be statistically significant.

Results

Cell morphology of primary simian and human macrophages

We compared the morphologic phenotype of human and macaque (*M. nemestrina*) monocytes using phase contrast microscopy (Fig. 2A and B). By the seventh day post-seeding, monocytes had fully differentiated

Table 2. Comparison of homology for various KP enzymes between rhesus macaque and human.

KP enzymes	Spieces	Accession	Size (basepair)	Homology (%)
IDO-1	*Macaca Mulatta*	NM001077483	1392	95
	Homo Sapien	NM-002164	1944	
TDO-2	*Macaca Mulatta*	XR_002804253	1551	95
	Homo Sapien	NM_005651.3	1703	
KAT-2	*Macaca Mulatta*	XM_001082463.2	1519	95
	Homo Sapien	NM_001008661.2	2165	
KYNU	*Macaca Mulatta*	XM_002798863.1	1463	95
	Homo Sapien	NM_001199241.1	1774	
KMO	*Macaca Mulatta*	XM_001093900.2	2361	90
	Homo Sapien	NM_003679.4	5266	
3-HAO	*Macaca Mulatta*	XM_001111024.2	1281	96
	Homo Sapien	NM_012205.2	1301	
QPRT	*Macaca Mulatta*	XM_001097266.2*	888*	96
	Homo Sapien	NM_014298.3	1575	
ACMSD	*Macaca Mulatta*	XM_001097996.2	1369	95
	Homo Sapien	NM_138326.2	1278	
GAPDH	*Macaca Mulatta*	NM_001195426.1	1106	97
	Homo Sapien	NM_002046.4	1401	

Table 3A. Primers sequences used to target KP enzymes for both simian and human cDNA.

Gene	Forward	Reverse	Band size	Temp. (°C)
1. IDO-1	ggcccaaagaagtttgcag	ggaagttcctgtgagctggt	160	60.0
2. TDO-2	cagacagtgccttttcacca	gtgcatccgagaaacaacct	367	60.8
3. KAT-2	tgcatcagcgatgaggttta	ttcttcagcagcatccagtg	621	59.7
4. KYNU	ggaagcgtccttggattaca	atcgtatgggcatgcttttc	589	60.8
5. KMO	ccaagcttcaatctgcacac	caaacggagttgattgctca	535	57.3
6. 3-HAO	aagaagcccctgtggtgac	cacaaacaggatgcccagta	506	59.7
7. QPRT	caactgccaagtctcctggt	ctccaccttcagagcgaagt	397	58.0
8. ACMSD	agctaccccaggaggtttgt	gcaaatggctatggtggtct	297	58.0
9. GAPDH	acccagaagactgtggatgg	cttggcaggtttttccagac	213	60.0

into macrophages. Not surprisingly, the macrophages were polymorphic with elliptical, round, or fusiform shapes. The cellular phenotype was relatively similar between macaque and human cell cultures. However, it was noted that simian macrophages were smaller in size compared to human macrophages which is consistent with the literature.[24] Confirmation in the purity of the macrophages using established markers, CD68 showed that >95% positive staining against DAPI was obtained (Fig. 2C–F).

Expression of KP genes by simian and human macrophages

There was higher amplification signal at 24 h post IFN-γ stimulation compared with 48 and 72 h (results not shown). Hence, only data from 24 h is presented hereafter. There were no detectable bands in the negative controls (PCR mix without cDNA) or in unstimulated macrophages at 24, 48 and 72 h (data not published). Strong IDO-1 expression was detected in all macrophage cultures, while KMO, KYNU, and 3HAO were moderately expressed (Fig. 3A). The remaining four KP enzymes, namely, TDO-2, KAT-2, ACMSD and QPRT were weakly expressed (Fig. 3A). Further analysis of the images based on optical density was performed to obtain the ratios of the KP enzyme mRNA expression normalized against the housekeeping gene GAPDH (Fig. 3B). It was noted that the mRNA expression patterns were consistent across all three macaque species and human macrophages. However, expression of ACMSD was lower in human macrophages compared to their simian counterparts (Fig. 3B).

We tested our primers for simian IDO-1 together with another set of published primers,[19] and obtained similar results in terms of mRNA expression (data not shown).

Table 3B. Summary of PCR run sequences.

Cycle repeats on step (2): 35	Temp. (°C)	Run time (min.)	Steps
Denaturation	94	4.5	1
Denaturation	94	1	2
Hybridization	Specify in Table 3A	1	
Extension	72	1.5	
Extension	72	10	3

Expression of KP enzymes in simian and human macrophages

Results from the ICC demonstrated that the expression of KP enzymes was detectable at the protein production level. IDO-1 and QUIN showed the strongest staining. KYNU and KMO stainings were of moderate intensity, while TDO-2, KAT-2, ACMSD and QPRT showed weaker signals. Staining was mainly perinuclear with some intra-cytoplasmic expansions (Fig. 4). As for RNA expression profile, staining patterns were similar between human (Fig. 4A) and simian macrophages (Fig. 4B and C).

Controls included (i) macrophages without IFN-γ stimulation, IFN-γ stimulated macrophages for 72 hrs with (ii) blocking solution (5% NGS in PBS), only secondary antibodies (monoclonal and polyclonal antibodies) and (iii) irrelevant IgG_1 primary monoclonal antibodies (Fig. 4E). All controls were negative validating the specificity of the staining.

De novo synthesis of KP metabolites in simian and human macrophages

Quantification of TRP and KYN by HPLC

In the supernatants collected from unstimulated human and simian macrophages, very little TRP

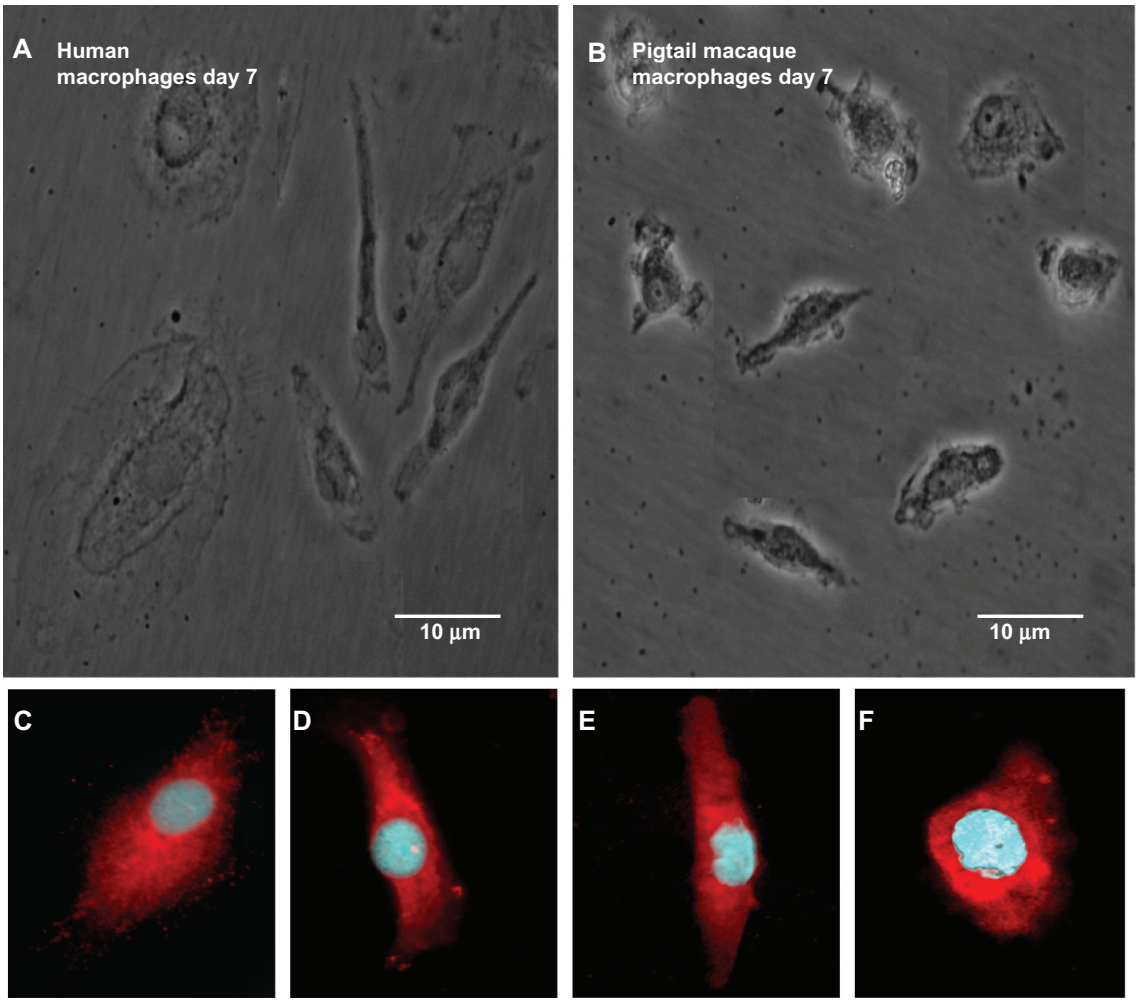

Figure 2. Macrophages cultures of human (**A**) and pigtail macaque (**B**) at 7 day in vitro. Pictures were taken with phase contrast microscope, at 400× magnification. Bar scale = 10 µm. Immunocytochemical stains for macrophage identification with surface marker, CD-68 on isolated (**C**) human, (**D**) pigtail macaque, (**E**) cynomolgus macaque and (**F**) rhesus macaque macrophage cultures.

catabolism or KYN production were detected at any time point. In contrast, following macrophage stimulation with IFN-γ, progressive significant ($P < 0.0001$) degradation of TRP with increased KYN levels was found at all three time points (Fig. 5A and B). On average, there was 47.68 ± 5.37 µM of TRP and 6.99 ± 0.77 µM of KYN in controls without IFN-γ stimulation over 24, 48 and 72 h. Following treatment by IFN-γ, TRP was rapidly degraded to concentration of 6.13 ± 3.49 µM, 7.51 ± 4.51 µM, and 3.49 ± 0.79 µM over 24, 48 and 72 h post stimulation, respectively, while KYN production was at concentration of 26.88 ± 3.29 µM, 44.78 ± 4.68 µM, and 52.47 ± 6.65 µM at 24, 48 and 72 h post stimulation, respectively.

Using the data from TRP and KYN levels, we calculated the KYN/TRP (K/T) ratio which indirectly estimates the activity of IDO-1 in macrophages (Fig. 5C). Parenthetically, PCR data indicate that TDO-2 expression is low (Fig. 3), suggesting that changes to the K/T ratio are likely due to IDO-1 stimulation. The changes in K/T ratio exhibit an average of a 10-fold increase at 24 h, a further 6-fold increase at 48 h and 3-fold increase at 72 h. In addition, we observed that the K/T ratio was higher in human macrophages at 72 h compared to their simian counterparts (Fig. 5C).

Quantification of QUIN and PIC by GC/MS

QUIN and PIC were constitutively produced by macrophages without IFN-γ stimulation at mean basal levels of 0.34 ± 0.04 µM and 0.32 ± 0.04 µM, respectively (Fig. 6). Following stimulation with IFN-γ, QUIN was progressively and significantly

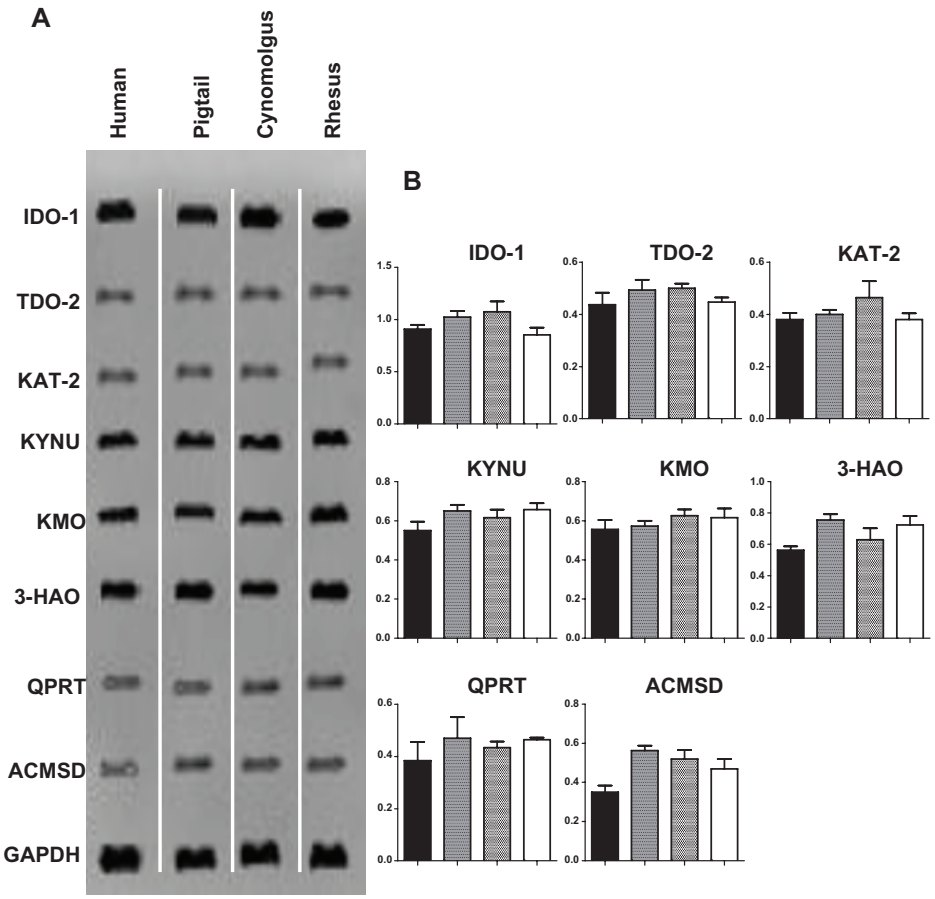

Figure 3. Expression of the kynurenine pathway enzymes using RT-PCR in macrophages stimulated with IFN-γ for 24 h. (**A**) Ethidium bromide-stained gels showing RT-PCR for IDO-1, TDO-2, KAT-2, KYNU, KMO, 3-HAO, QPRT, ACMSD and GAPDH expression (top to bottom). The first column corresponds to human macrophages, the second to pigtail macaque macrophages, the third to cynomolgus macaque macrophages and fourth to rhesus macaque macrophages. (**B**) The histograms indicate the ratio of the expression of the eight kynurenine pathway enzyme mRNA relative to the GAPDH mRNA expression. Each column of the histogram also corresponds to the columns in (**A**).
Note: Individual samples were analyzed in triplicate, and the SEM for all data was determined to be ±7%.

increased to 0.87 ± 0.11 μM (24 h), 1.38 ± 0.17 μM (48 h), and 2.05 ± 0.26 μM (72 h) illustrated in Figure 6A. In addition, when QUIN was analyzed with baseline normalization, the production of QUIN in IFN-γ-stimulated macrophages was 2.5-fold, a further 3.8-fold, and a further 6-fold increment at 24, 48 and 72 h, respectively. There was a declining trend with production of PIC in succession over first 48 h after IFN-γ stimulation in simian macrophages but not in human cells (Fig. 6B). However, a significant decrease in the production of PIC after 72 h was observed in both human and simian macrophages culture ($P < 0.0001$) stimulated with IFN-γ (Fig. 6B). The mean PIC concentrations for IFN-γ stimulated macrophages were 0.29 ± 0.07 μM (24 h), 0.2 ± 0.07 μM (48 h), and 0.09 ± 0.03 μM (72 h). Analyses of all samples were carried out in triplicate.

Discussion

The main aim of this study was to characterize the KP in primary macrophages from three different macaque species in order to assess the relevance of studying KP in simian models of human physiology or pathology.

IDO-1 is known to be strongly induced by IFN-γ and play key roles in the immune response regulation[25] while TDO-2 is more often associated with metabolic changes.[26] The first similarity between human and simian macrophages is the induction of simian macrophages by human IFN-γ. This contrasts with murine macrophages that are only responsive to mouse IFN-γ but not human IFN-γ. This is reflected by the semi-quantitative RT-PCR data showing a strong increase in expression of mRNA IDO-1 expression whereas TDO-2 was only weakly expressed (<0.4 fold increase) (Fig. 3). High levels of mRNA expression

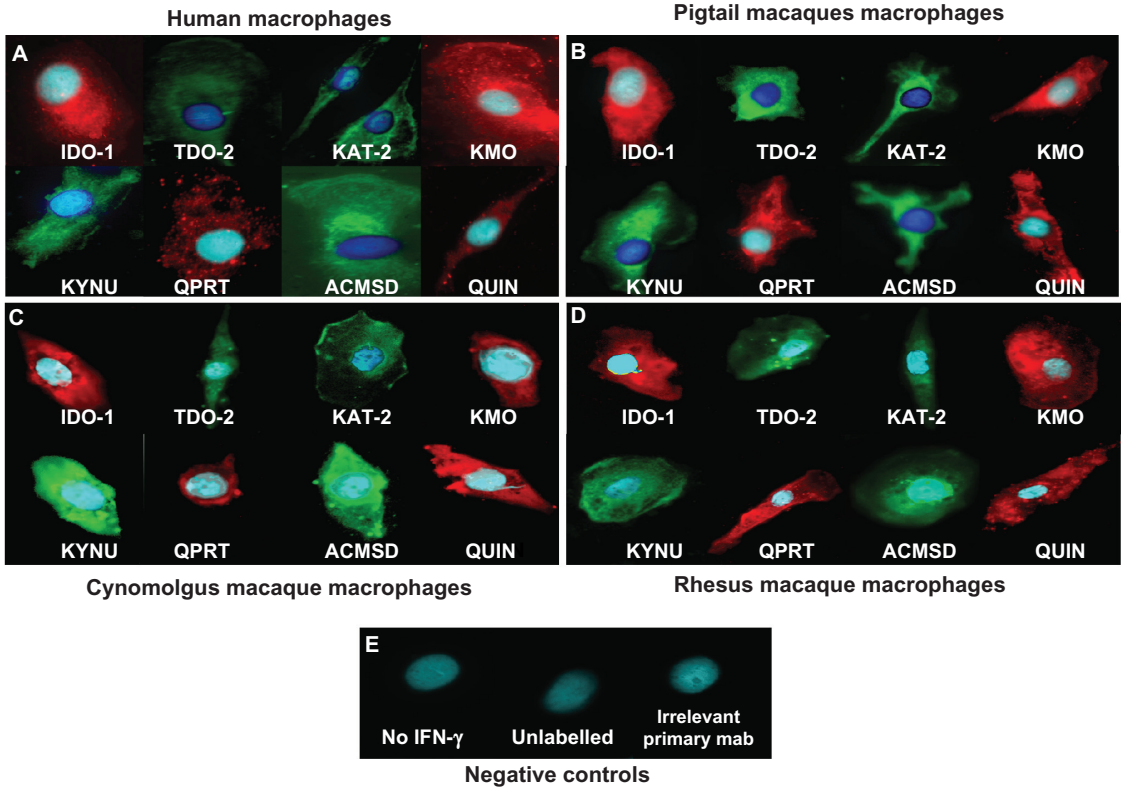

Figure 4. Immunodetection of various KP enzymes and QUIN in (**A**) human, (**B**) pigtail macaque, (**C**) cynomolgus macaque and (**D**) rhesus macaque macrophages. (**E**) Control preparations of cultures of human macrophages: without IFN-γ stimulation, without antibodies (unlabelled), irrelevant primary antibodies and secondary antibodies only.

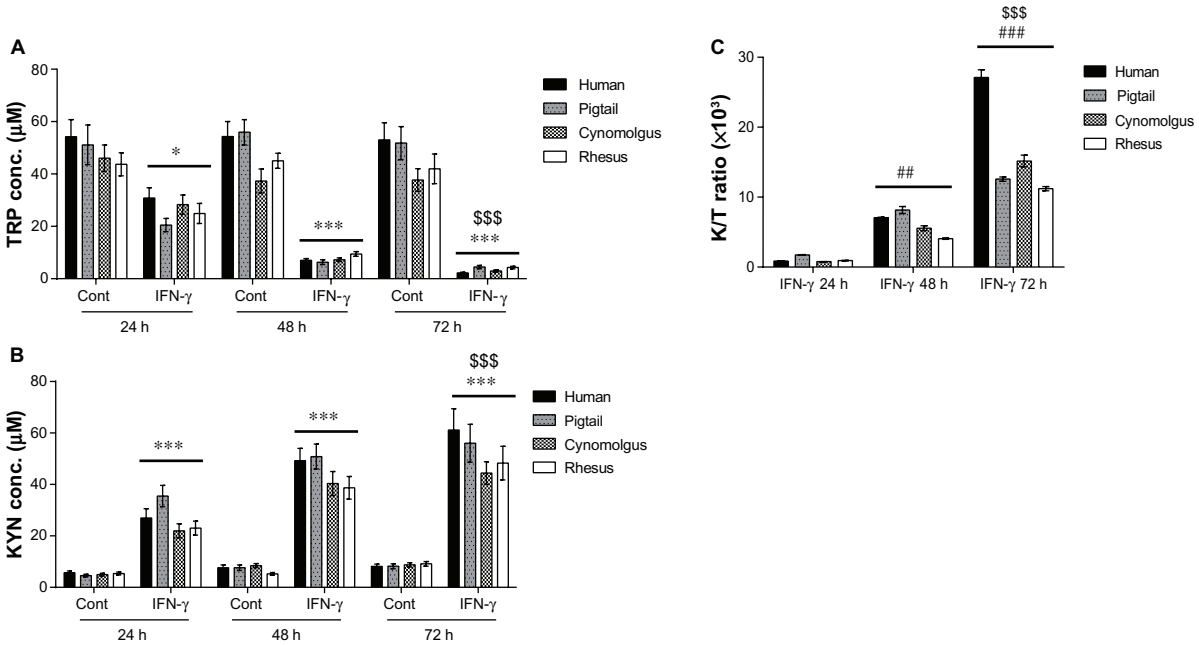

Figure 5. Histogram showing levels of tryptophan (**A**) kynurenine (**B**) and the level of KP activation reflected by K/T ratio (**C**) in human and simian macrophages using HPLC.
Notes: Controls (Cont) were untreated macrophages cultures whereas interferon-γ (IFN- γ) stimulated macrophages were treated for 24, 48 and 72 h. Only IFN-γ stimulated macrophages cultures for 24, 48 and 72 h results were presented in (C) to illustrate KP activation in time-dependent manner to IFN-γ stimulation. Statistical differences comparing (i) the untreated and its counterpart IFN-γ-treated conditions are denoted by *; (ii) the changes in concentration to 24 h time point are denoted by # and; (iii) the change in concentration detected at the 48 or 72 h compared to 24 h time point are denoted by $. One-symbol, two-symbol and three-symbols are indicated as $P < 0.05$; $P < 0.01$ and $P < 0.0001$, respectively (Dunnett's test).

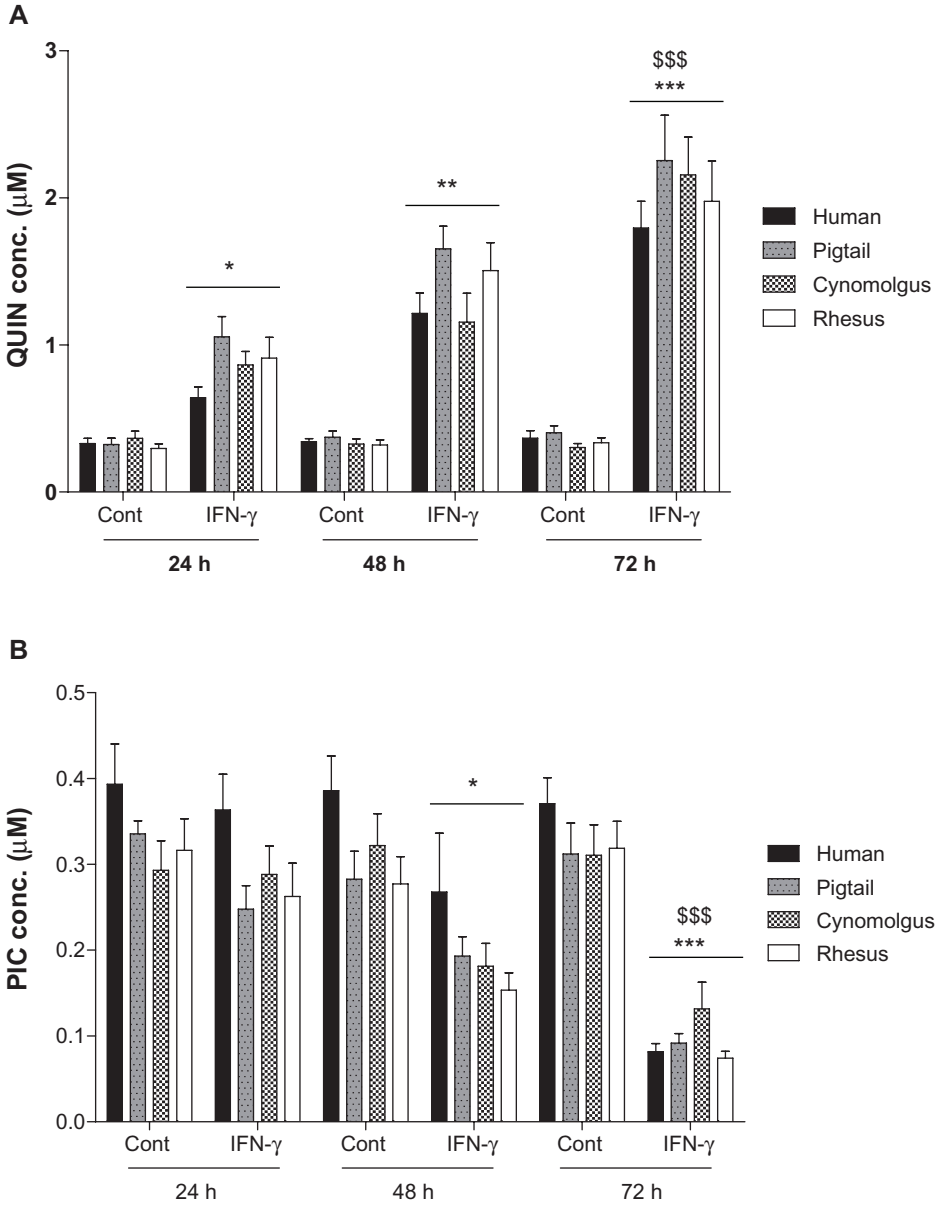

Figure 6. Histogram showing de novo synthesis of quinolinic acid (QUIN; **A**) and picolinic acid (PIC; **B**) in human and simian macrophages using GCMS.
Notes: Control (Cont) were untreated macrophages cultures whereas interferon-γ (IFN-γ) stimulated macrophages were treated for 24, 48 and 72 h. Statistical differences comparing the untreated and its counterpart IFN-γ-treated conditions are denoted by * whereas the change in concentration detected at the 48 or 72 h compared to 24 h time point are denoted by $. One-symbol, two-symbol and three-symbol are indicated as $P < 0.05$; $P < 0.01$ and $P < 0.0001$, respectively (Dunnett's test).

of IDO-1 were also associated with significant conversion of TRP to KYN in immune stimulated cells in comparison to control (Fig. 5C). However, further analysis of the IDO-1 activity between species showed that human IDO-1 activity was higher in human cells than in macaque cells at 72 h (Fig. 5C), possibly reflecting a better biological activity of rhIFN-γ toward human versus simian macrophages. IDO-1 activity was similar among the 3 studied macaque species. We noticed that although small amounts of KYN, QUIN, and PIC were detected in the supernatant of unstimulated macaque MdM cultures (without IFN-γ), no mRNA or protein expression was detected using RT-PCR or ICC, suggesting that the level of expression was below our limit of detection. This low level of activation of the macrophage cultures is probably due to the culture medium containing serum and/or adhesion on plastic.

In accordance with a previous review[27] describing the KP in human and murine monocytic lineages, the

KAT-2 expression does not appear to be significantly affected by immune stimulation in macaque macrophages, further committing the pathway to switch towards the production of QUIN at the branching point of 3-HK and KYNA production. Furthermore, other midstream enzymes such as KYNU, KMO, and 3-HAO had a higher level of expression (~0.6–0.8 fold increase) compared to KAT-2. ACMSD is considered to be neuroprotective as it plays a key role in regulating PIC biosynthesis and limiting the generation of neurotoxic QUIN.[8,28] However, during immune stimulation, ACMSD expression remains low, probably leading to a higher non-enzymatic conversion of ACMS to QUIN. The overall effect of the increased IDO-1 activity with low ACMSD and QPRT activity leads to an increased production of QUIN by macaque macrophages. This is confirmed by our data showing an accumulation of QUIN and a low amount of PIC (Fig. 6). This is also in accordance with previous studies[6,29,30] using human macrophages. We found that the mRNA expression of the KP enzymes reached its highest at 24 h compared to 48 h and 72 h (results not shown), whereas for protein production the highest levels were detected at 72 h. This is in agreement with our previous studies.[6,31] The immunodetection of protein expression of the KP enzymes in macaque macrophages correlated well with the production of their corresponding KP metabolites (data not shown).

Previously, it has been shown that human macrophages produce approximately 20- to 30-fold more QUIN than microglia.[29,31,32] Our data for QUIN are in accordance with an earlier study showing a time-dependent increase of QUIN in primary cultures of human macrophages stimulated with 100 IU/mL of IFN-γ.[32] In this earlier study, Heyes et al[32] found a 2.8-fold increase in QUIN production between unstimulated and IFN-γ stimulated macrophage cultures at 24 h and a 3-fold increase at 48 h. Our results show a similar trend with 2.4-fold and 3.8-fold increase in QUIN levels from IFN-γ stimulated macaque macrophage cultures at 24 and 48 h, respectively. Accordingly, this was also observed in our previous study looking at various cytokines treatments in human macrophages.[4]

All the above data suggest that macaque macrophages may be relevant *in vitro* models to study QUIN production and inflammation in human pathology.[33] This study further supports previous one demonstrating QUIN accumulation[18] in SIV infected macaque models mimicking human AIDS dementia complex.[19] We previously showed that human macrophages are the main source of QUIN and this is likely to be similar in the macaque models, resulting in QUIN accumulation during inflammation. However, it was also noted that the KP metabolism in serum and CSF could be significantly different between species. For example, Fujigaki et al[12] compared KYN and anthranilic acid in serum and CSF of human, macaques, rabbit, rats, and guinea pigs and found that the levels of these metabolites were very different between species, particularly rat and rabbit.

Some technical considerations need to be highlighted. A variety of methodologies used in different laboratories and the different ways of reporting data may hinder the comparisons with other previous studies. Another factor complicating the interpretation of *in vitro* data is the presence of variable concentrations of KP metabolites, including QUIN, in the different batches of serum added to culture media. It has been reported that QUIN concentrations can range from 80 nM to 4.89 μM in commercially available sera. Therefore the baseline amount of QUIN can be higher than expected.[34] Thus, comparison of the actual level of de novo synthesis of KP metabolites such as KYN, PIC, and QUIN as well as the level of TRP degradation in various *in vitro* models remains a challenge and will require further validation using serum-free and/or KP metabolite-free media.

Conclusions

This study represents the first comprehensive characterization of the KP in macaque and human macrophages. We found a high degree of similarity in the expression of KP enzymes (IDO-1, TDO-2, KAT-2, KYNU, KMO, 3-HAO, ACMSD, and QPRT) and de novo synthesis/degradation of KP metabolites (TRP, KYN, QUIN, and PIC) between macrophages from humans and three different species of macaques. This was further illustrated by the presence of similar positive staining for all the KP enzymes in human and simian macrophages using immunodetection (Fig. 4). Our data validate the macaque models as a relevant approach to study the human cellular KP metabolism in the context of inflammation. This suggests that simian macrophages can be used as an *in vitro* model to test KP inhibitors or siRNA targeting the human KP

enzymes provided that these are verified to overcome the minute interspecies variations that still remain.

Our present results further suggest that macaques may allow in vivo proof-of-concept for efficacy and specificity of newly designed inhibitors targeting the KP.[35] Moreover, as macaques are widely used as a model for AIDS and ADC,[36] our *in vitro* model will be of particular interest for investigating macrophage infection by HIV and its multiple interactions with the immune system in which the KP plays a key role.

Acknowledgement

The authors wish to acknowledge the Bioanalytical Mass Spectrometry Facility at UNSW for their kind support, especially Ms Sonia Bustamante for her technical expertise and kind advice with the GC/MS. The authors will also like to thanks Prof. Osamu Takikawa and Prof. Christine Miller for their generous provision of IDO-1 and TDO-2 antibodies, respectively.

Author Contributions

Conceived and designed the experiments: GJG, MMCY, BJB. Analyzed the data: GJG, CKL, MMCY. Wrote the first draft of the manuscript: CKL. Contributed to the writing of the manuscript: GJG, BJB. Agree with manuscript results and conclusions: GJG, BJB, SJK, GG. Jointly developed the structure and arguments for the paper: BS, JCB, RDR, BH. Made critical revisions and approved final version: GJG, BJB, SJK, GG, CKL. All authors reviewed and approved of the final manuscript.

Funding

This work was funded by University of New South Wales, St. Vincent's Clinic Foundation, the Australia National Health and Medical Research Council, the Curran Foundation and Australian Research Council.

Competing Interests

Author(s) disclose no potential conflicts of interest.

Disclosures and Ethics

As a requirement of publication the authors have provided signed confirmation of their compliance with ethical and legal obligations including but not limited to compliance with ICMJE authorship and competing interests guidelines, that the article is neither under consideration for publication nor published elsewhere, of their compliance with legal and ethical guidelines concerning human and animal research participants (if applicable), and that permission has been obtained for reproduction of any copyrighted material. This article was subject to blind, independent, expert peer review. The reviewers reported no competing interests.

References

1. Braidy N, Grant R, Brew BJ, Adams S, Jayasena T, Guillemin GJ. Effects of kynurenine pathway metabolites on intracellular nad+ synthesis and cell death in human primary astrocytes and neurons. *Int J Tryptophan Res*. 2009;2:61–9.
2. Munn DH, Zhou M, Attwood JT, et al. Prevention of allogeneic fetal rejection by tryptophan catabolism. *Science*. 1998;281(5380):1191–3.
3. Heyes MP, Chen CY, Major EO, Saito K. Different kynurenine pathway enzymes limit quinolinic acid formation by various human cell types. *Biochem J*. 1997;326(Pt 2):351–6.
4. Pemberton LA, Kerr SJ, Smythe G, Brew BJ. Quinolinic acid production by macrophages stimulated with IFN-gamma, TNF-alpha, and IFN-alpha. *J Interferon Cytokine Res*. 1997;17(10):589–95.
5. Kerr SJ, Armati PJ, Guillemin GJ, Brew BJ. Chronic exposure of human neurons to quinolinic acid results in neuronal changes consistent with AIDS dementia complex. *AIDS*. 1998;12(4):355–63.
6. Guillemin GJ, Kerr SJ, Smythe GA, et al. Kynurenine pathway metabolism in human astrocytes: a paradox for neuronal protection. *J Neurochem*. 2001;78(4):842–53.
7. Guillemin GJ, Wang L, Brew BJ. Quinolinic acid selectively induces apoptosis of human astrocytes: potential role in AIDS dementia complex. *J Neuroinflammation*. 2005;2:16.
8. Guillemin GJ, Cullen KM, Lim CK, et al. Characterization of the kynurenine pathway in human neurons. *J Neurosci*. 2007;27(47):12884–92.
9. Allegri G, Bertazzo A, Biasiolo M, Costa CV, Ragazzi E. Kynurenine pathway enzymes in different species of animals. *Adv Exp Med Biol*. 2003;527:455–63.
10. Allegri G, Costa CV, Bertazzo A, Biasiolo M, Ragazzi E. Enzyme activities of tryptophan metabolism along the kynurenine pathway in various species of animals. *Farmaco*. 2003;58(9):829–36.
11. Croitoru-Lamoury J, Lamoury FMJ, Caristo M, et al. Interferon-γ Regulates the Proliferation and Differentiation of Mesenchymal Stem Cells via Activation of Indoleamine 2,3 Dioxygenase (IDO). *PLoS ONE*. 2011;6:e14698.
12. Fujigaki S, Saito K, Takemura M, et al. Species differences in L-tryptophan-kynurenine pathway metabolism: quantification of anthranilic acid and its related enzymes. *Arch Biochem Biophys*. 1998;358(2):329–35.
13. Saito K, Quearry BJ, Saito M, Nowak TS Jr., Markey SP, Heyes MP. Kynurenine 3-hydroxylase in brain: species activity differences and effect of gerbil cerebral ischemia. *Arch Biochem Biophys*. 1993;307(1):104–9.
14. Heyes MP, Saito K, Chen CY, et al. Species heterogeneity between gerbils and rats: quinolinate production by microglia and astrocytes and accumulations in response to ischemic brain injury and systemic immune activation. *J Neurochem*. 1997;69(4):1519–29.
15. Saito K, Markey SP, Heyes MP. Effects of immune activation on quinolinic acid and neuroactive kynurenines in the mouse. *Neuroscience*. 1992;51(1):25–39.
16. Jauch DA, Sethy VH, Weick BG, Chase TN, Schwarcz R. Intravenous administration of L-kynurenine to rhesus monkeys: effect on quinolinate and kynurenate levels in serum and cerebrospinal fluid. *Neuropharmacology*. 1993;32(5):467–72.

17. Depboylu C, Reinhart TA, Takikawa O, et al. Brain virus burden and indoleamine-2,3-dioxygenase expression during lentiviral infection of rhesus monkey are concomitantly lowered by 6-chloro-2′,3′-dideoxyguanosine. *Eur J Neurosci.* 2004;19(11):2997–3005.
18. Weed MR, Hienz RD, Brady JV, et al. Central nervous system correlates of behavioral deficits following simian immunodeficiency virus infection. *J Neurovirol.* 2003;9(4):452–64.
19. Burudi EM, Marcondes MC, Watry DD, Zandonatti M, Taffe MA, Fox HS. Regulation of indoleamine 2,3-dioxygenase expression in simian immunodeficiency virus-infected monkey brains. *J Virol*. 2002;76(23):12233–41.
20. Cohen J. AIDS research. Vaccine studies stymied by shortage of animals. *Science.* 2000;287:959–60.
21. Batten CJ, De Rose R, Wilson KM, et al. Comparative evaluation of simian, simian-human, and human immunodeficiency virus infections in the pigtail macaque (Macaca nemestrina) model. *AIDS Res Hum Retroviruses.* 2006; 22(6):580–8.
22. Kerr SJ, Armati PJ, Pemberton LA, Smythe G, Tattam B, Brew BJ. Kynurenine pathway inhibition reduces neurotoxicity of HIV-1-infected macrophages. *Neurology*. 1997;49(6):1671–81.
23. Smythe GA, Braga O, Brew BJ, et al. Concurrent quantification of quinolinic, picolinic, and nicotinic acids using electron-capture negative-ion gas chromatography-mass spectrometry. *Anal Biochem*. 2002;301(1):21–6.
24. Krombach F, Munzing S, Allmeling AM, Gerlach JT, Behr J, Dorger M. Cell size of alveolar macrophages: an interspecies comparison. *Environ Health Perspect.* 1997;105(Suppl 5):1261–3.
25. Takikawa O. Biochemical and medical aspects of the indoleamine 2,3-dioxygenase-initiated L-tryptophan metabolism. *Biochem Biophys Res Commun.* 2005;338(1):12–9.
26. Hayaishi O. Musajo memorial award lecture: metabolism to function—an odyssey with tryptophan. *Adv Exp Med Biol*. 2003;527:1–11.
27. Schwarcz R. The kynurenine pathway of tryptophan degradation as a drug target. *Curr Opin Pharmacol*. 2004;4(1):12–7.
28. Tanabe A, Egashira Y, Fukuoka S, Shibata K, Sanada H. Expression of rat hepatic 2-amino-3-carboxymuconate-6-semialdehyde decarboxylase is affected by a high protein diet and by streptozotocin-induced diabetes. *J Nutr*. 2002;132(6):1153–9.
29. Espey MG, Chernyshev ON, Reinhard JF Jr., Namboodiri MA, Colton CA. Activated human microglia produce the excitotoxin quinolinic acid. *Neuroreport*. 1997;8(2):431–4.
30. Guillemin GJ, Smith DG, Kerr SJ, et al. Characterisation of kynurenine pathway metabolism in human astrocytes and implications in neuropathogenesis. *Redox Rep.* 2000;5(2–3):108–11.
31. Guillemin GJ, Smith DG, Smythe GA, Armati PJ, Brew BJ. Expression of the kynurenine pathway enzymes in human microglia and macrophages. *Adv Exp Med Biol.* 2003;527:105–12.
32. Heyes MP. Quinolinic acid in culture media used for in vitro neurotoxicology studies. *Neurosci Lett*. 1992;145(2):234–5.
33. Guillemin GJ. Quinolinic acid, the inescapable neurotoxin. *FEBS J*. 2012; 279:1356–65.
34. Heyes MP, Saito K, Markey SP. Human macrophages convert L-tryptophan into the neurotoxin quinolinic acid. *Biochem J*. 1992;283(Pt 3):633–5.
35. Samadi P, Gregoire L, Rassoulpour A, et al. Effect of kynurenine 3-hydroxylase inhibition on the dyskinetic and antiparkinsonian responses to levodopa in Parkinsonian monkeys. *Mov Disord.* 2005;20(7):792–802.
36. Williams KC, Corey S, Westmoreland SV, et al. Perivascular macrophages are the primary cell type productively infected by simian immunodeficiency virus in the brains of macaques: implications for the neuropathogenesis of AIDS. *J Exp Med*. 2001;193(8):905–15.